Electric Power Systems Research 157 (2018) 157–167

Contents lists available at ScienceDirect

Electric Power Systems Research

journal homepage: www.elsevier.com/locate/epsr

Utilizing synchrophasor-based supplementary damping control signals in conventional generator excitation systems

M.S. Almas [a,*], M. Baudette [a], L. Vanfretti [b]

[a] SmarTS-Lab, Department of Electric Power and Energy Systems, KTH Royal Institute of Technology, Osquldas vag 10, Stockholm SE-11428, Sweden
[b] Rensselaer Polytechnic Institute, Department of Electrical, Computer, and Systems Engineering, 110 Eighth Street, Troy, NY 12180-3590, USA

ARTICLE INFO

Article history:
Received 6 May 2017
Received in revised form 4 December 2017
Accepted 5 December 2017
Available online 27 December 2017

Keywords:
Damping control
Excitation Control System
Latency compensation
Phasor measurement units
Power System Stabilizer
Real-Time Hardware-in-the-Loop simulation
Synchrophasors

ABSTRACT

A supplementary function of Excitation Control Systems (ECSs) for synchronous generators is that of a Power System Stabilizer (PSS). The PSS implementation in these ECSs only allows the use of a limited type of pre-defined local input measurements and built-in PSS algorithms. To adapt existing ECSs to take advantage of synchrophasors technology, this paper proposes and implements a prototype wide-area damping controller (WADC) that provides synchrophasor-based damping input signals to existing ECSs. The developed WADC comprise (i) a real-time mode estimation module, (ii) synchrophasor's communication latency computation module, and (iii) phasor-based oscillation damping algorithm executing in a real-time hardware prototype controller.

Through Real-Time Hardware-in-the-Loop (RT-HIL) simulations, it is demonstrated that synchrophasor-based damping signals from the WADC can be utilized together with a commercial ECS, thus providing new options for selection of the best feedback signal for oscillation damping.

1. Introduction

In addition to synchronous generator's terminal voltage regulation, a commercial Excitation Control System (ECS) [1] may also provide Power System Stabilizer (PSS) functions to damp power system oscillations [2]. Small disturbances may result in undamped oscillations in a heavily loaded interconnected power system [3]. Undamped oscillations, if not mitigated, result in loss of synchronism of one or a group of machines from the rest of the power system and may lead to a system collapse [4].

Different vendors have deployed diverse PSS types in their ECS units, which can be configured to provide damping for power system oscillations. These built-in PSSs utilize single or multiple *local* input measurements (e.g. rotor speed, rotor angle deviation and generator's accelerating power) to damp oscillations. These input measurements are pre-configured and cannot be modified by the user. The user must tune the available pre-defined parameters to provide oscillation damping. These configurations have to be deployed locally at the power plant and cannot be modified remotely by the system operators.

With the deployment of Phasor Measurement Units (PMUs) in the power grid, there is a possibility of utilizing wide-area measurements for enhancing real-time detection and control of small-signal instability [5,6].

1.1. Paper motivation

With the currently available commercial ECS, power system operators cannot exploit wide-area measurements from PMUs as an input damping signal to generator AVRs. This is primarily because the ECS's are not yet capable of exploiting synchrophasor technology.

However, there is a possibility to disable the ECS's PSS function and instead supply it with PMU-based external damping signals configured as an analog input to the commercial ECS at the internal AVR's summing junction.

1.2. Literature review

Power system researchers, over the years, have demonstrated through power system simulation studies, the effectiveness of PMU-based wide-area measurements for power oscillation damping (POD) [6–14]. These wide-area measurements may provide better observability of inter-area modes which might not be available in local signals utilized by conventional damping controllers.

* Corresponding author.
E-mail addresses: msalmas@kth.se (M.S. Almas), baudette@kth.se (M. Baudette), vanfrl@rpi.edu (L. Vanfretti).

https://doi.org/10.1016/j.epsr.2017.12.004
0378-7796/

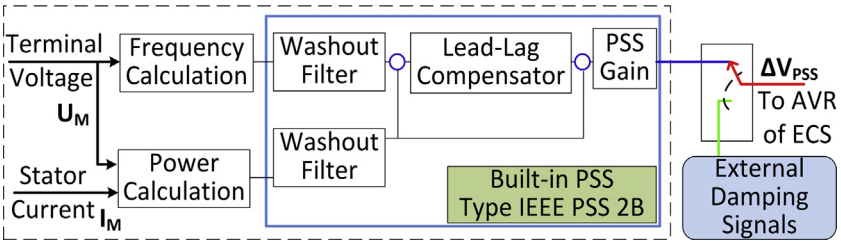

Fig. 1. Model of the PSS incorporated in Unitrol 1020 ECS.

Even though the prospects of wide-area damping control implementations are quite promising, to the knowledge of the authors, there are relatively very few of such deployments in the field. One pilot test was carried out in the Norwegian power system utilizing voltage phase angle measurements from PMUs as reported in Ref. [15]. This WADC provides damping signals to the voltage regulator of a Static Var Compensator (SVC). Although the field trials were successful, they were insufficient to conclude whether the WADC performs more satisfactorily than the local measurement-based damping controller. The design and testing of a WADC in China Southern Power Grid (CSG) is reported in Ref. [16]. This WADC utilizes PMU measurements as its input and modulates two HVDC systems for power system damping. Even though the closed-loop field testing of CSG's WADC was successful, it remains in open-loop trial operation mode to further study its impact on system's dynamics. A WADC hardware prototype controller is currently undergoing open-loop testing at the Bonneville Power Administration (BPA) synchrophasor laboratory as reported in Ref. [17]. This WADC utilizes PMU measurements to calculate frequency difference between two areas, which is used to compute a directional power command used to modulate the controllers for oscillation damping.

The above mentioned WADC systems have been implemented as supplementary controls for Flexible AC Transmission Systems (FACTS) or HVDC systems to damp oscillations. Although these deployments are valuable advances for oscillation damping, their realization requires either a new installation of FACTS/HVDC system or to modify the existing control loops in order to support both local (conventional) signals and PMU-based signals. Note that the number of FACTS and HVDCs in today's power system is relatively small and installing such a system for the sole purpose of oscillation damping is not economically sound [18]. Furthermore, utilizing wide-area measurement based control loops on FACTS/HVDC systems together with the existing PSSs of a commercial ECS may result in interference between the controllers, which is not desirable [19,20].

As many of the ECSs of large generators are equipped with built-in PSSs, it is attractive to explore the possibility of providing wide-area based external damping signals to these ECS while minimizing changes to the existing installations and the ECS itself.

1.3. Paper contributions

The goal of this paper is to demonstrate the utilization and effectiveness of supplying synchrophasor-based external damping signals to a commercial ECS for oscillation damping. The presented approach utilizes wide-area measurements from PMUs to generate damping signals, which are fed to the commercial ECS as an analog input. The novelty of the approach is that it utilizes the existing ECS installation without making any substantial changes to it and/or its associated electrical installation. In addition, this approach allows the user to select the input signals utilized to generate the damping signal, and allows remote tuning of the controller parameters before supplying them to the ECS. Therefore, the proposed approach can be used to generate damping signals adaptive to the changes in operating conditions or network topology, which can be configured remotely (e.g. by TSOs).

1.4. Paper organization

The paper is organized as follows: Section 2 provides information about ABB's Unitrol 1020 ECS and its PSS functionality. Section 3 presents the proposed synchrophasor-based WADC prototype to provide external damping signals to the ECS. The hardware interface and the RT-HIL experimental setup used for experimental testing are shown in Section 4. Performance assessment of the ECS when coupled to the WADC is compared against its internal PSS in Section 5, while the results are discussed in Section 6. In Section 7, conclusions are drawn.

2. Unitrol 1020 ECS overview

2.1. Unitrol 1020 Excitation Control System

Unitrol 1020 is an automatic voltage regulator (AVR) that provides excitation control of indirectly excited synchronous machines and rotors [21]. The primary purpose of the device is to maintain the generator's terminal voltage while taking into account all the operational limits of the generator.

2.2. PSS feature of Unitrol 1020 excitation system

The PSS feature available in Unitrol 1020 ECS is described by the IEEE Std. 421.5-2005 PSS 2A/2B model [22] and its representation is shown in Fig. 1. The PSS2B type has a dual structure that uses two *local* signals (rotor speed "ω" and power "P").

This built-in PSS is usually tuned once (during commissioning) for a specific electromechanical oscillatory mode, through design methods [23] that rely on linear power system models (i.e. for a limited range of system's operating conditions). Once tuned, the PSS settings can only be modified locally at the power generation station, where the ECS is located. This limits the ability of TSOs to calibrate PSS settings to adapt to changes in system.

3. PMU-based WADC

3.1. Oscillation damping algorithm/function

The damping algorithm used in the proposed WADC was first proposed in Ref. [24] and is shown in Fig. 2. For illustrative purposes, consider a measurement signal that contains both a change in the average and the onset of an oscillation. This signal can be described as:

$$u(t) = u_{pref} + \Delta u_{av} e^{-\frac{t-t_{event}}{T_{av}}} + \Delta u_{osc} e^{-\frac{t-t_{event}}{T_{osc}}} \cos\left(\Omega t + \varphi_{osc}\right) \quad (1)$$

$$u(t) = U_{av} + \left\{\bar{U}_{osc} e^{j\Omega t}\right\} \quad (2)$$

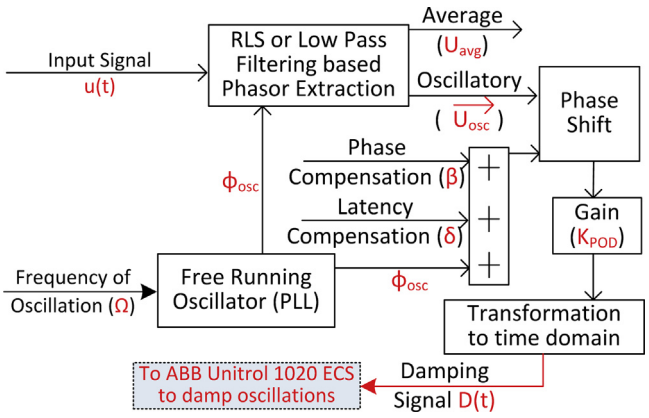

Fig. 2. Operating principle of damping algorithm implemented.

where u_{pref} is pre-fault signal (steady-state), Δu_{avg} is the change in input signal, t_{event} is the disturbance event time, T_{av} is the time constant of the average signal, Δu_{osc} is the oscillation amplitude, Ω is the oscillation frequency and φ_{osc} is the phase of the oscillation. Using Eq. (2), the average and oscillatory content of the measured signal can be defined as;

$$U_{av} = u_{pref} + \Delta u_{av} e^{-\frac{t-t_{event}}{T_{av}}} \tag{3}$$

$$\vec{U}_{osc} = \Delta u_{osc} e^{-j\Omega t_{event}} e^{j\varphi_{osc}} \tag{4}$$

The main objective of the algorithm in Fig. 2 is to separate the oscillatory content of the input signal ($\vec{U}_{osc}$) from its average value (U_{av}). This can be achieved by using either a recursive least square estimation technique or a low pass filter [24]. The oscillatory part of the measured input signal is extracted as a complex phasor ($\vec{U}_{osc}$) that represents the signal oscillating in coordinate system, which rotates with oscillatory frequency (Ω). The damping signal is computed by applying a phase shift and gain on the extracted oscillatory phasor signal. Hence, the damping signal produced by the phasor POD algorithm is represented as:

$$D(t) = \left(K_{POD}\vec{U}_{osc}e^{j\beta}\right) e^{j\Omega t} \tag{5}$$

where K_{POD} is the gain and β is the desired phase shift.

3.2. WADC software and hardware implementation

This section provides detail of the different modules of the developed WADC. The information flow from receiving the synchrophasor stream in the workstation to the generation of the damping signal is shown in Fig. 3. Below is the description of each module.

3.2.1. M1: synchrophasor-data parsing module

To receive synchrophasor measurements in the WADC, a protocol parser [25] is used in a workstation. The protocol parser establishes a data socket to receive the incoming synchrophasor stream and unwraps it according to IEEE C37.118.2 protocol [26]. The raw numerical values of the phasors, analogs and digitals wrapped in the synchrophasor streams are made available in the LabVIEW environment.

3.2.2. M2: power system mode estimation module

To identify the critical oscillatory modes in the system, the parsed synchrophasor data is received from M1 in a real-time mode estimation module (M2). Two estimation algorithms; one for ambient data and one for ring-down data are implemented in this module. The mode estimator utilizes stochastic state-space subspace identification (SSSID) [27] for estimating modes through ambient measurements, while Eigensystem Realization Algorithm

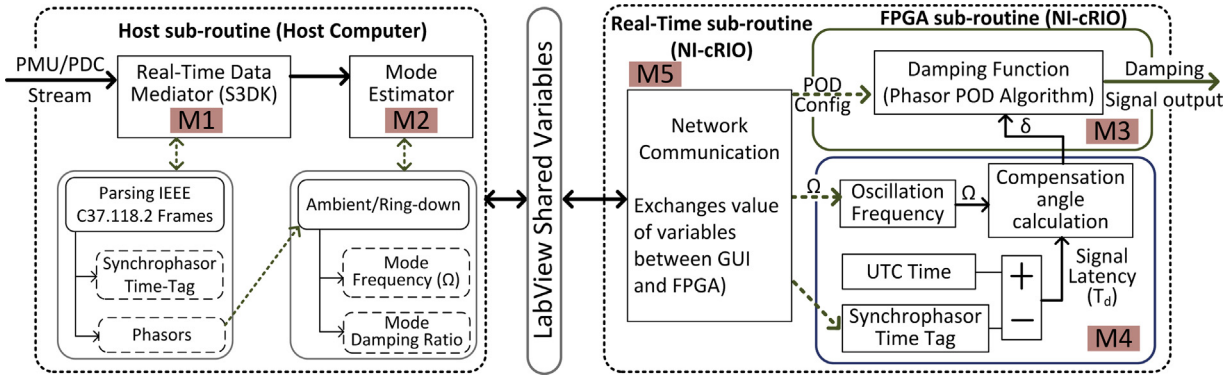

Fig. 3. Information flow between various modules of the developed WADC.

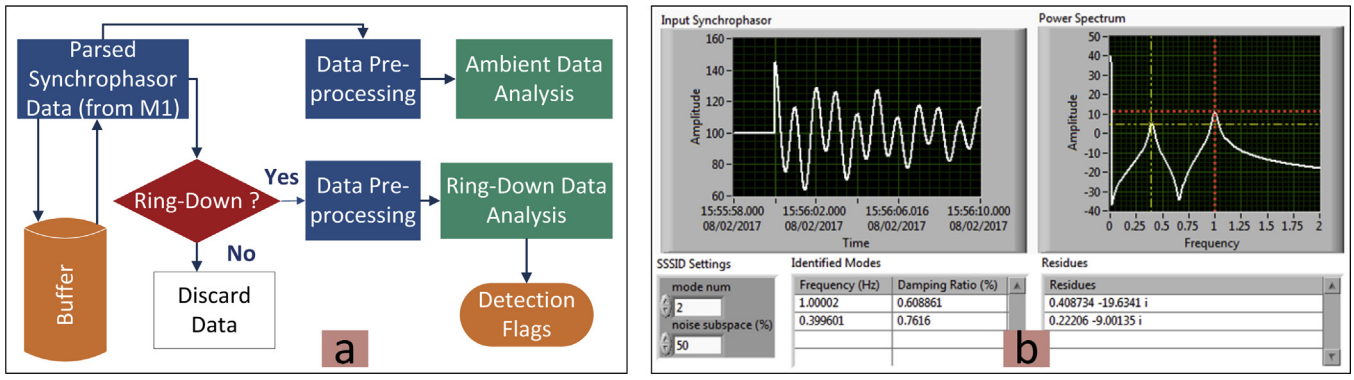

Fig. 4. Mode estimation module of the developed WADC (M2).

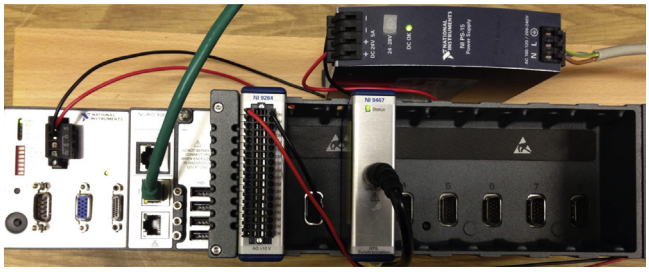

Fig. 5. Phasor-POD algorithm executing on NI-cRIO 9082 RT controller showing an NI-9264, analog output module and NI-9467, GPS module.

(ERA) is used to extract critical modes through ring-down analysis [28]. The modular architecture of the mode estimation application is shown in Fig. 4a, whereas Fig. 4b shows the frequency and damping estimation from the ring-down data algorithm for the test signal. The design and testing of this real-time mode estimator application is reported in Ref. [29]. This module performs the following tasks; (i) receives real-time parsed synchrophasor measurements as input, (ii) pre-processes these measurements before supplying them to the estimation algorithms, and (iii) outputs frequency (Ω) and damping ratio of the estimated modes. The frequency of the estimated modes is fed to the subsequent modules in WADC to generate damping signals.

3.2.3. M3: oscillation damping algorithm module

The Phasor-POD algorithm is deployed in a National Instrument's Compact Reconfigurable Input/Output (NI-cRIO 9082) real-time controller [30]. To ensure deterministic and quick response time from the controller, the damping algorithm is executed on the FPGA of the NI-cRIO. The FPGA of the NI-cRIO can incorporate parallel Phasor-POD algorithms, each configured to damp a different oscillatory frequency. Therefore, this WADC architecture is flexible and scalable to damp multiple oscillatory modes. The complete architecture of this module is reported in Ref. [31].

This module receives information regarding (i) frequency (Ω) of the estimated modes from M2, and (ii) phase angle off-set (δ) for communication latency compensation computed by M4. The output of the algorithm i.e. the damping signal $D(t)$ is directly written to the analog output module (NI-9264) of the NI-cRIO. The damping signals are received from the analog output module (NI-9264) and fed to the ECS as analog inputs. Fig. 5 shows the hardware prototype of the WADC.

3.2.4. M4: communication latency compensation

To compute the communication latency in the feedback control loop, the WADC is synchronized with the GPS through a GPS time-stamping and synchronization module (NI-9467). The WADC computes the signal latency (T_d) by subtracting the instant of origin at the PMU from that of arrival at the WADC. This is shown in Fig. 6. As the electric power system relies on GPS signals for time synchronization and it is readily available in the substation/generation-sites, it is therefore practical to use such a scheme for accurately computing wide-area signal latency.

Based on the computed latency (T_d) and the frequency of oscillatory mode (Ω) computed through real-time mode estimator, the WADC calculates the phase angle off-set (δ) using Eq. (6) to compensate for the communication latency in the received synchrophasor measurement.

$$\delta = 360^0.\Omega.T_d \tag{6}$$

This module executes in the FPGA of the NI-cRIO and provides phasor-POD algorithm (M3) with the information of phase angle off-set (δ). This information is used by M4 to generate communication latency compensated damping signal. The GUI of this module is shown in Fig. 7 where the average communication latency of the synchrophasor test signal is 164 ms. This GUI also displays critical information such as GPS status and location of the WADC.

3.2.5. M5: data mediation between host computer and NI-cRIO

This module handles communication between the host computer where the protocol parser (M1) and mode estimation (M2) is executed, and the WADC functions executing in the FPGA of NI-cRIO, which includes oscillation damping (M3) and communication latency computation (M4). This allows for monitoring and selection of the damping algorithm's inputs, visualizing WADC output and analyzing the resource utilization of the NI-cRIO.

3.3. WADC's remote access and configuration

To facilitate TSOs in selecting and configuring the WADC to adapt to changes in operating conditions and network topology, the Graphical User Interface (GUI) of the WADC, shown in Fig. 8, is made accessible to the users through the LabVIEW Web Publishing Tool [32]. This feature allows hosting a "Remote Front Panel" in the form of webpage on the real-time (RT) target (NI-cRIO 9082), thus waiving the requirement of a dedicated server.

As shown in Fig. 8, the remote front panel allows selecting synchrophasor measurements from the synchrophasor dataset to be used as an input for the damping algorithm. This selection can be made through a scroll down menu option labelled as "i". Once the synchrophasor input is selected, the GUI populates its field "ii" with average signal latency (T_d) of the selected synchrophasor which is computed by M4. The frequency of oscillatory modes (Ω) estimated by M2 appears in the field labelled as "iii". The oscillation damping algorithm's parameters such as desired phase shift (β) and gain (K_{POD}) can be configured through the controls labelled as "iv" and "v", respectively. The phase angle offset (δ) for communication latency compensation is displayed in the field labelled as "vi". The GUI of the WADC enables the operator to monitor the real-time performance of the damping algorithm in the form of the plots, as shown in Fig. 8(vii–x).

To make this application secure so that it is only accessible and configurable by authorized personnel (e.g. TSOs), 2-step protection is enabled. The first protection is implemented by explicitly setting the IP addresses that can access the webpage hosting GUI of WADC. The IP addresses not on the authorized list are unable to access the GUI. Second protection is implemented through credential checks. This assures that even if the webpage is accessible, the personnel will not be able to proceed past the login screen without a valid password.

4. RT-HIL experimental setup

4.1. RT-HIL experimental setup

In order to demonstrate the proposed WADC and investigate the performance of the Unitrol 1020 ECS when provided with external damping signals, a 2-area 2-machine power system was modeled in the MATLAB/Simulink environment using the SimPowerSystems Toolbox and configured for RT-HIL simulation. The single line diagram of the test model and the overall experimental setup is shown in Fig. 9. The test system consists of two areas linked together by a 500 kV/700 km transmission line. Area-1 and Area-2 are equipped with a salient-pole synchronous generator rated 13.8 kV/1000 MVA and 13.8 kV/5000 MVA, respectively. The load is split between the areas in such a way that Area-1 is exporting 915 MW power to Area-2. The system is stable under steady-state. However, when a small perturbation in the form of a 5% magnitude step at the voltage reference of the AVR of generator G2 is applied for 10 cycles, it results

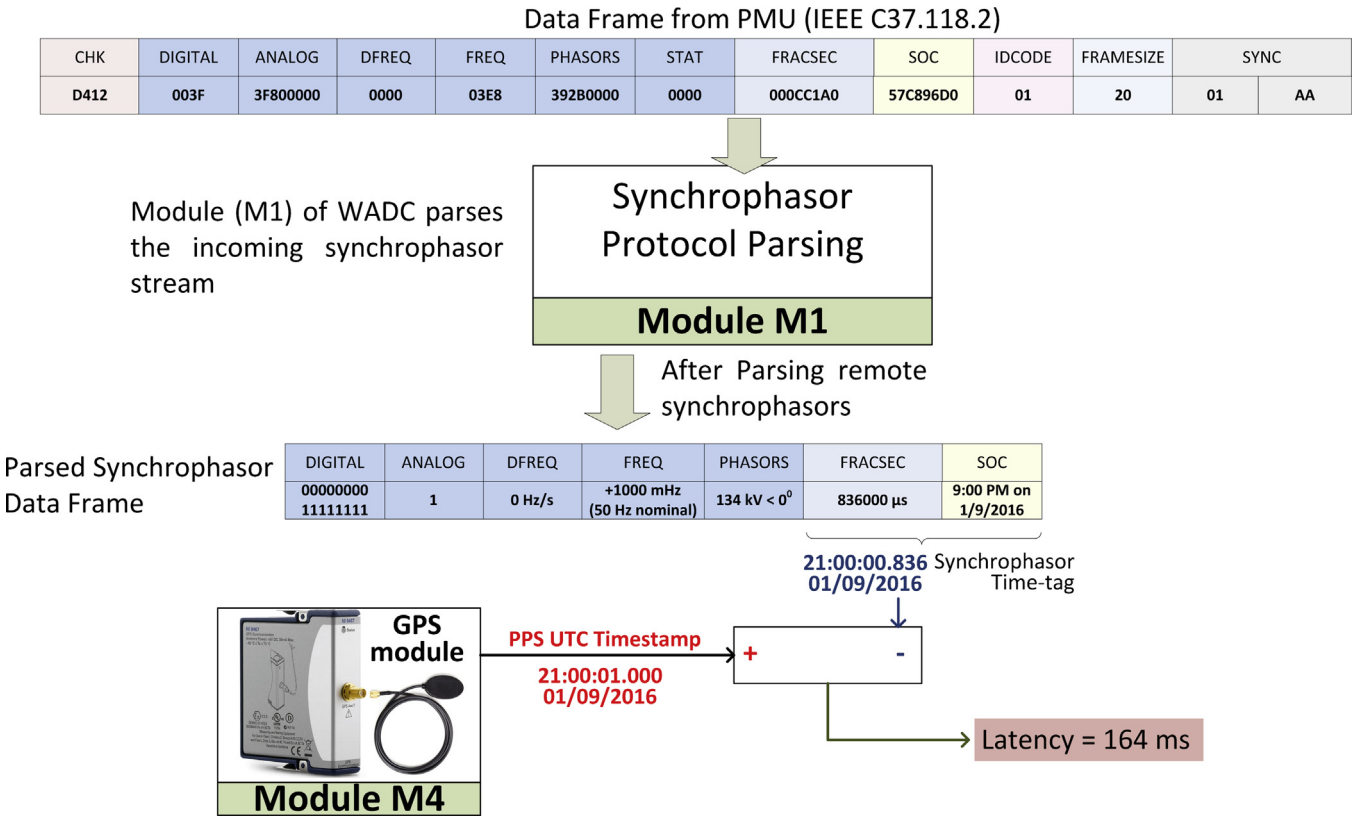

Fig. 6. Communication latency computation module (M4) of WADC.

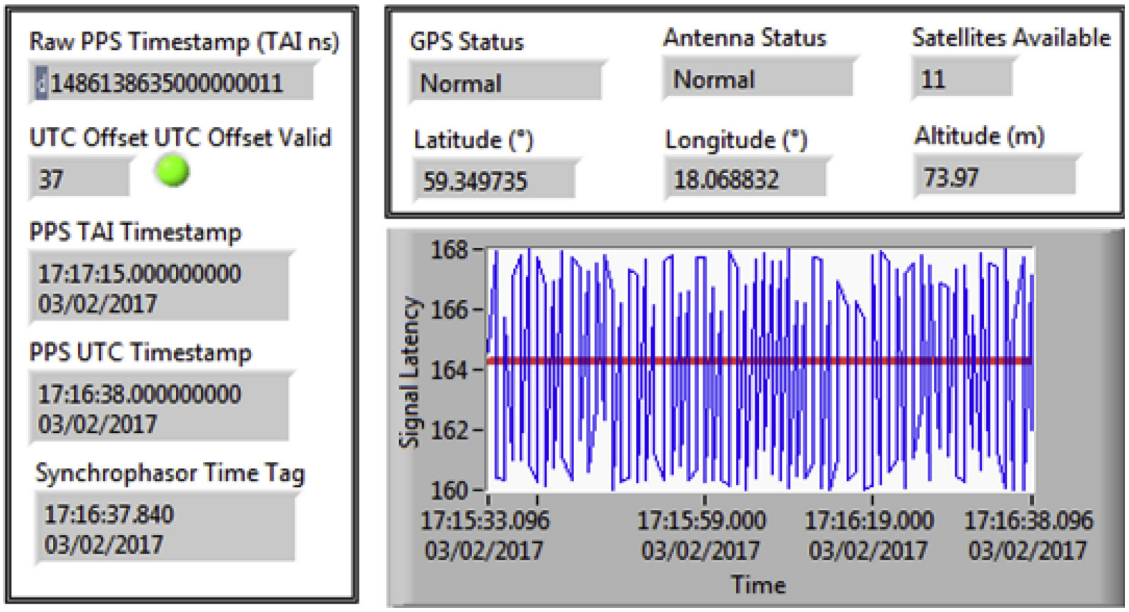

Fig. 7. GUI of communication latency computation module (M4).

in an undamped inter-area mode of 0.91 Hz. The excitation control of generator G1 is supplied through the Unitrol 1020 ECS with its internal PSS function disabled and configured to receive external damping signals through its analog inputs. The field voltage of G2 is supplied through an IEEE Type-1 DC1A exciter [22] without a stabilizing function (PSS disabled).

Therefore, the damping for inter-area oscillations is provided by Unitrol 1020 ECS at G1 using the external damping signals which are received through the WADC. The workflow enabled by the experimental setup shown in Fig. 9 is described as follows.

1. The test system is executed in real-time using Opal-RT's eMEGAsim Real-Time Simulator [33].
2. Three phase currents and voltages from Bus 1 and Bus 2 are amplified and fed to CTs and VTs of PMUs.

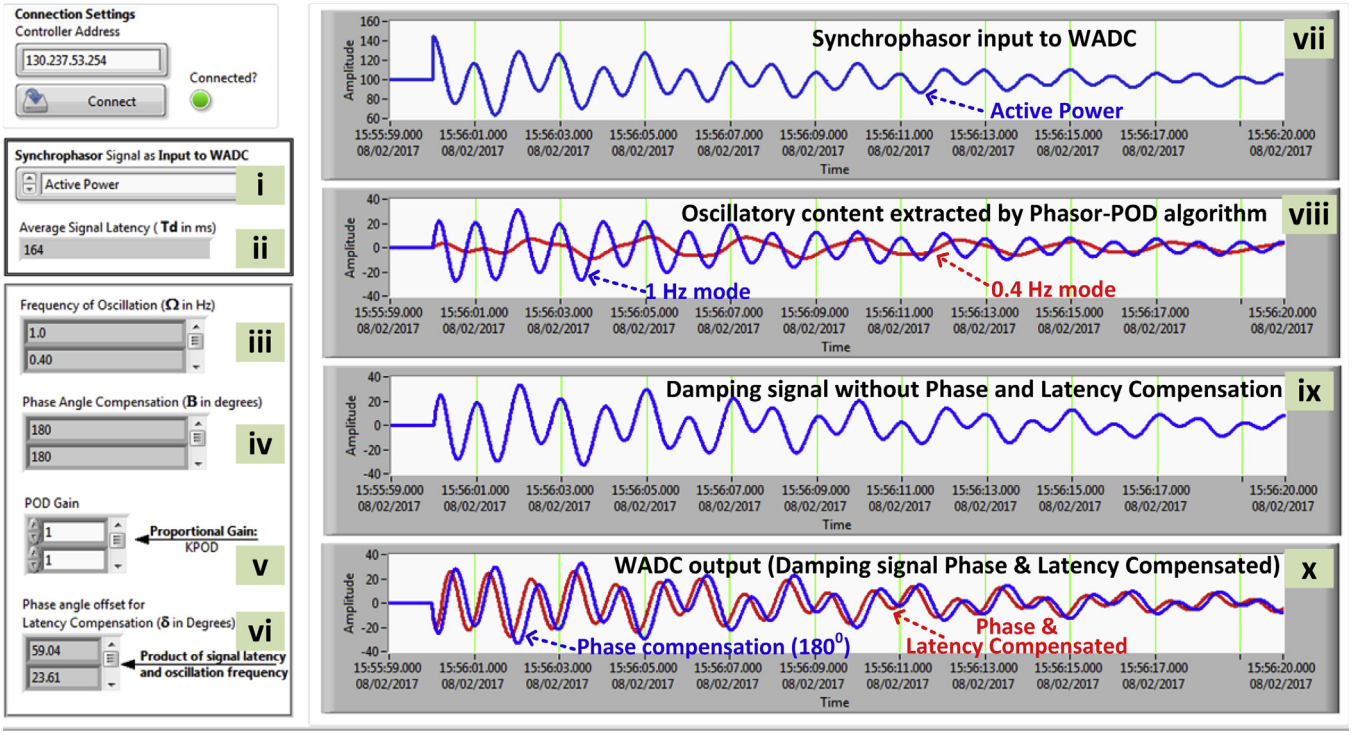

Fig. 8. GUI of the WADC published over the network and accessible through a web-browser.

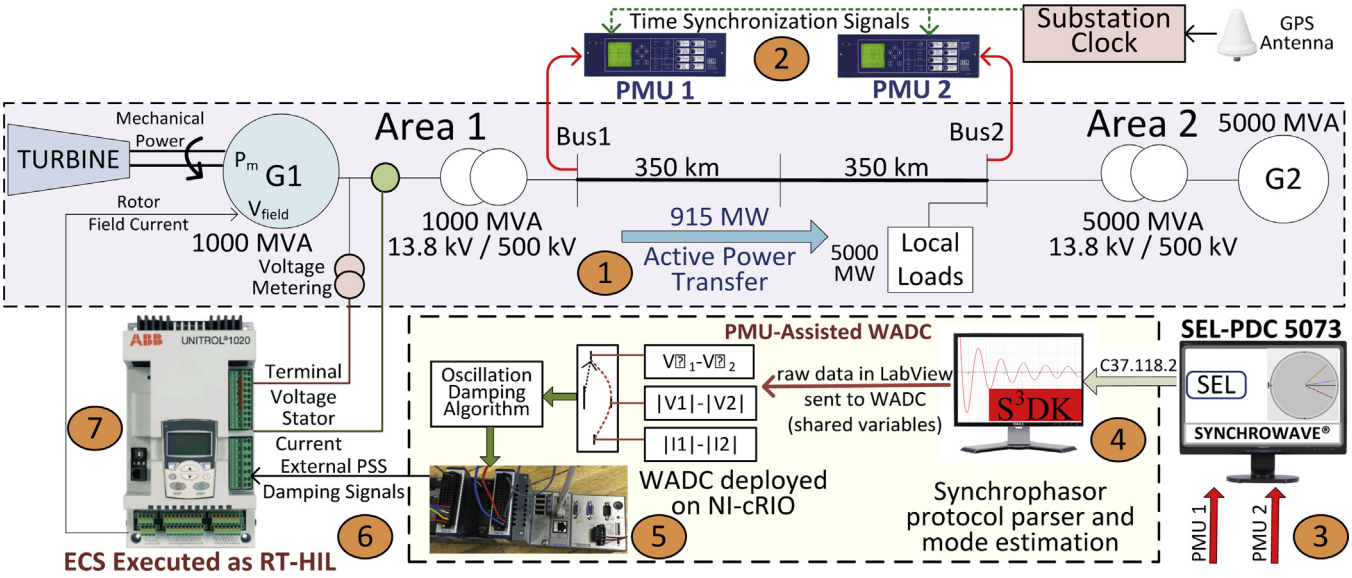

Fig. 9. Single line diagram of 2-area 2-machine power system model. Only generator G1 is equipped with the Unitrol 1020 ECS.

3. Synchrophasor streams from both PMUs are concentrated through a Phasor Data Concentrator (PDC).
4. A protocol parser (M1) unwraps this PDC stream and provides raw numerical values of all the phasors available in the stream in LabVIEW [25]. Frequency and damping estimates of the modes are computed by the mode estimation module (M2).
5. The raw synchrophasor measurements and frequency estimates of the modes are accessed by the WADC using shared variables [32]. The WADC executes the damping algorithm (M3) using the desired input synchrophasor measurement in real-time and generates a damping signal that is made available through one of the output channels of its output module (NI-9264).
6. This damping signal is fed to the Unitrol 1020 ECS as an analog input and is utilized internally in the ECS at the AVR's internal summing junction.
7. The excitation control signals from the ECS are fed to generator G1 executing in the RTS in real-time.

4.2. Interfacing the ECS with the RTS and WADC

The ECS is interfaced with the RTS and the WADC as shown in Fig. 10. The RTS only provides voltages and currents within ±10 V and ±20 mA, respectively. In order to make these signals compatible with the inputs of Unitrol 1020 ECS, the low-level signals of generator's G1 terminal voltage and stator current are boosted

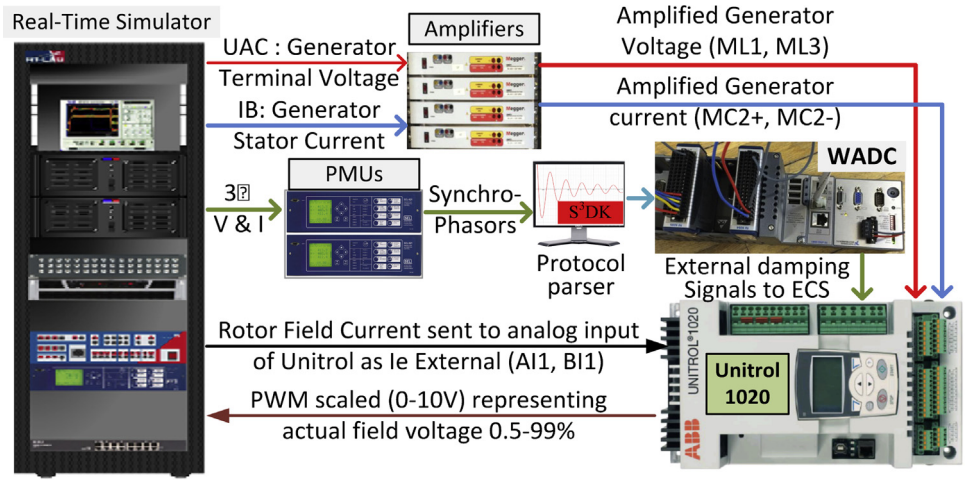

Fig. 10. Interfacing Unitrol 1020 ECS with Opal-RT simulator and WADC.

using linear amplifiers to 100 V and 1 A at rated power. The field current measurement of G1 is supplied to the ECS using low-level outputs (±10 V) and one of the inputs of the ECS is configured for receiving these excitation current measurements.

The damping signal generated from the WADC is accessed through its output module (NI-9264) and is fed as an analog input to the ECS. This is achieved by configuring the corresponding analog inputs of the ECS to receive external signals. Through the ECS configuration software, the hardware was configured to receive the analog input from the WADC (external damping signals) and utilize them as primary stabilizing signal to the ECS. During the experimental tests presented below, the primary stabilizing signal was toggled between its internal built-in PSS and the external damping signal from the WADC to perform comparative analysis.

5. Experimental testing

5.1. Case A: single inter-area mode & fixed signal latency

For this case, the experimental setup shown in Fig. 9 is used. When a small perturbation in the form of 5% magnitude step at the voltage reference of the AVR of generator G2 is applied for 10 cycles at t = 30 s, it results in an undamped inter-area oscillation of 0.91 Hz as shown in Fig. 11 (dotted trace). Next, the same scenario is repeated but this time the internal PSS of the ECS is tuned to damp this inter-area oscillation. This results in damping of the 0.91 Hz mode which is shown in Fig. 11 (red trace). Finally, the internal PSS of the ECS is bypassed and the damping signals are provided to the ECS externally through the WADC.

This set of experiments were carried out using the following synchrophasor input signals: (i) *Active Power* transfer between Area-1 and Area-2, (ii) *Positive Sequence Voltage Magnitude Difference* between two areas (|ΔV|), (iii) Positive Sequence *Voltage Phase Angle Difference* between two areas (Δθ), and (iv) *Positive Sequence Current Magnitude Difference* between the two areas (|ΔI|).

For this experiment, the signal latency from source (PMUs) to destination (NI-cRIO) as computed by latency computation module (M4) is 155 ms. This corresponds to a phase angle off-set (δ) of 50.8^0 to compensate for the communication latency in the received synchrophasor measurement. Appropriate phase shift (β) and the gain of the WADC (K_{POD}) configured when using each input signal to provide adequate damping are shown in Table 1. The experimental results are shown in Fig. 11, whereas, the time-domain performance metrics are shown in Table 2.

Table 1
Case A: parameter configuration of POD algorithm (single mode).

Parameter	WADC active power	WADC |ΔV|	WADC |Δθ|	WADC |ΔI|
Phase Shift (β)	90^0	180^0	90^0	90^0
Gain (K_{POD})	0.002	2	0.03	0.17

Table 2
Case A: time domain performance metrics (single mode).

Damping signal	Decay ratio	Overshoot (%)	Rise time (s)	Setting time (s)
Built-in PSS	0.961	8.09	1.02	4.68
WADC active power	0.966	10.61	1.00	5.14
WADC |ΔV|	0.969	11.08	0.96	6.46
WADC Δθ	0.947	11.70	0.36	4.02
WADC |ΔI|	0.971	11.95	0.98	5.64

5.2. Case B: single inter-area mode & variable signal latency

To investigate the performance of WADC when supplied with input signals with varying communication latency, the same scenario as in Case A is repeated. However this time, the communication latency of the input signal to the WADC is varied by configuring the "waiting period" in the PDC. For demonstration purpose, positive sequence voltage phase angle is used as an input signal to the WADC. The performance is assessed by first disabling the latency computation module (M4) of the WADC and incorporating signal latency of 50 ms, 100 ms, 150 ms and 200 ms in the WADC's input signal. As next step, the latency computation module (M4) is enabled and the signal with 200 ms of communication latency is used as an input. The results in Fig. 12 shows that the WADC adapts to the communication latency and effectively compensates it to provide power oscillation damping as opposed to the adverse impact when latency compensation is not accounted for.

5.3. Case C: damping of multiple oscillaotry modes

In order to analyze the performance of the ECS to damp multiple oscillatory modes when provided with external stabilizing signals from the WADC, the power system model shown in Fig. 13 is used. The model is similar to that of Fig. 9 with the following difference: G1 and G3 together with Load L1 constitute Area-1 which is linked to Area-2 through 500 kV/700 km transmission line. When a small perturbation in the form of a 5% magnitude step at the voltage reference of the AVR of G2 is applied for 10 cycles at t = 10 s, it results in the following oscillatory modes;

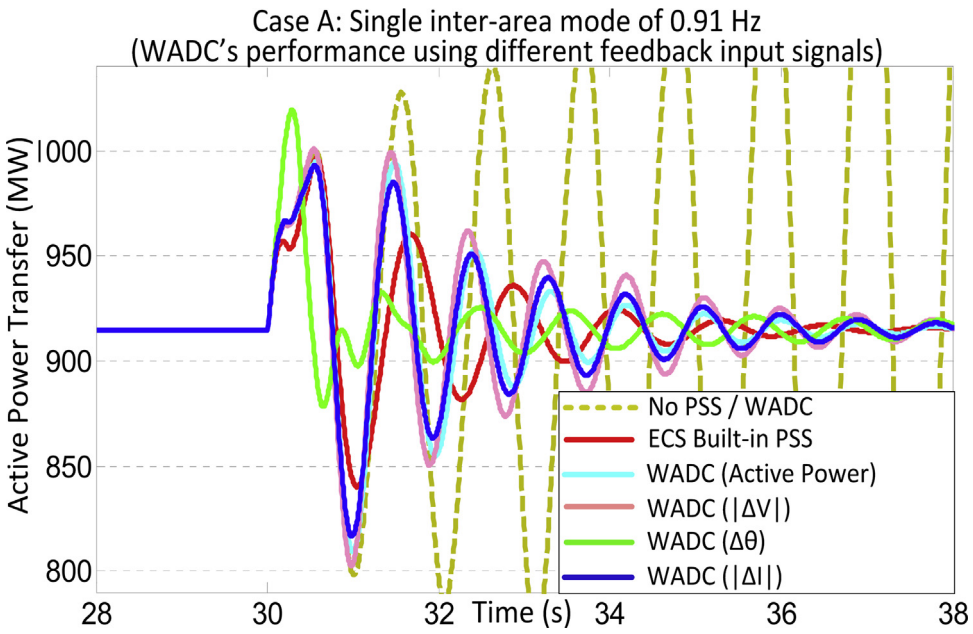

Fig. 11. Experimental results: 0.91 Hz inter-area mode damping using the internal-PSS and external damping signals from the WADC. (For interpretation of the references to color in the text, the reader is referred to the web version of this article.)

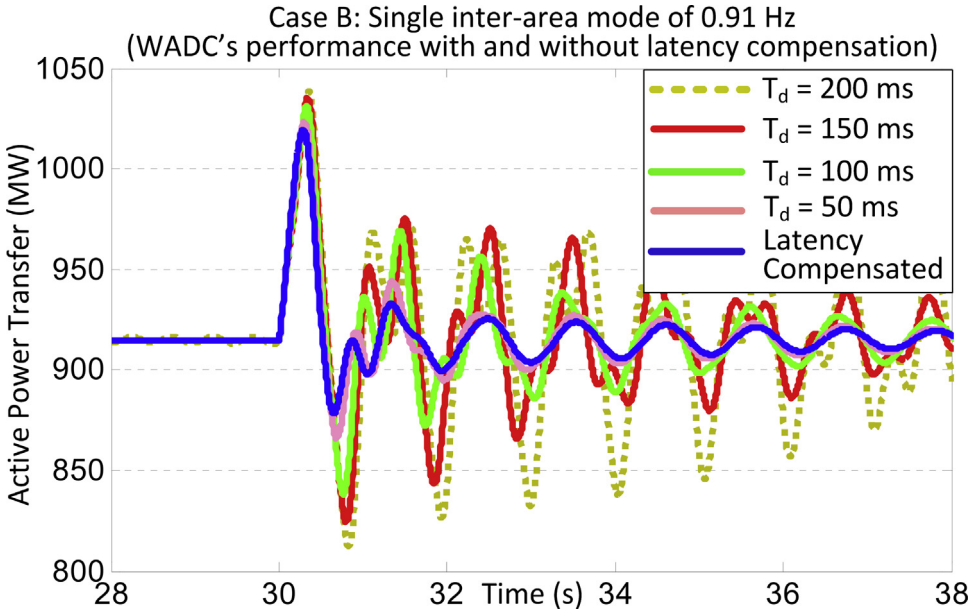

Fig. 12. Experimental results: 0.91 Hz inter-area mode damping in presence of different synchrophasor signal latency.

(1) Interarea-mode of 0.5 Hz involving the whole of Area-1 oscillating against Area-2.
(2) Local mode of Area-1 of 1.2 Hz involving this area's machines (G1 and G3) oscillating against each other.

Fig. 14 illustrates the experimental results of damping multiple oscillatory modes (1.2 Hz and 0.5 Hz) using the internal PSS and the external damping signals from the WADC. The response of the built-in PSS (tuned to damp 1.2 Hz local mode) is shown in Fig. 14 (red trace). The following signals were utilized to carry out experiments using external damping signals from the WADC: (i) *Active Power* transfer between two areas, (ii) *Positive Sequence Voltage Magnitude Difference* (|ΔV|), and (iii) Positive Sequence *Voltage Phase Angle Difference* between two areas (Δθ).

For this experiment, the signal latency computed by latency computation module (M4) is 180 ms. This implies a phase angle off-set of $\delta_1 = 32.4^0$ (corresponding to 0.5 Hz inter-area mode) and $\delta_2 = 77.8^0$ (corresponding to 1.2 Hz local mode) to compensate for the communication latency in the received synchrophasor measurement. The phase shifts (β_1, β_2) and the gain of the WADC (K_{POD1}, K_{POD2}) configured when using each input signal to provide adequate damping (for this scenario) are shown in Table 3 whereas, the time-domain performance metrics are shown in Table 4.

6. Results analysis

As shown in Figs. 11 and 14, in absence of any internal or external damping signal to the AVR of the ECS, the systems become unstable. The built-in PSS of the ECS provides adequate damping when there

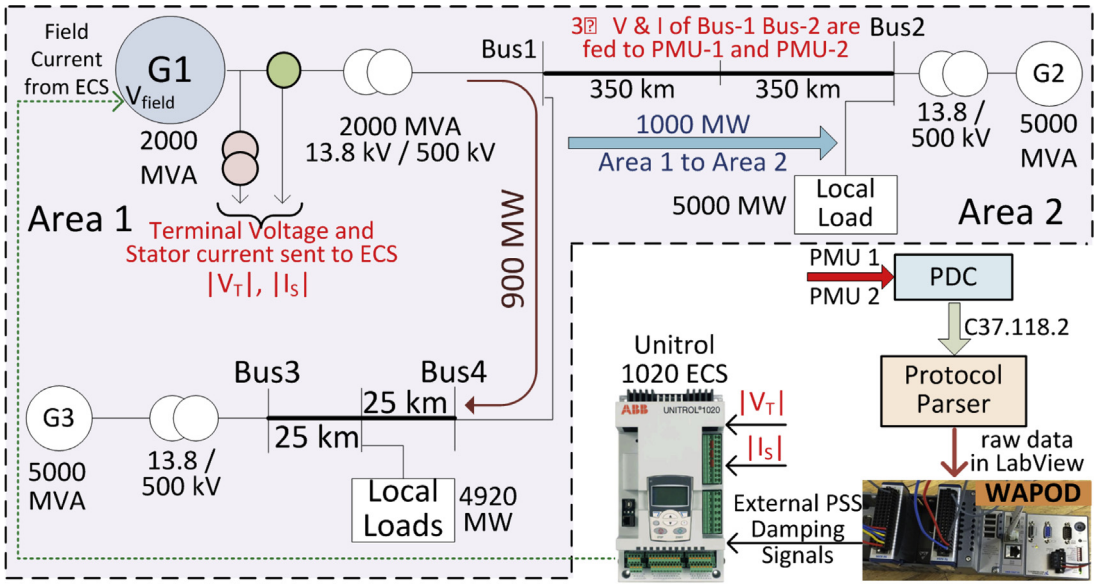

Fig. 13. Single line diagram of a 2-area 3-machine system. G1 is equipped with the Unitrol 1020 ECS receiving damping signals from the WADC.

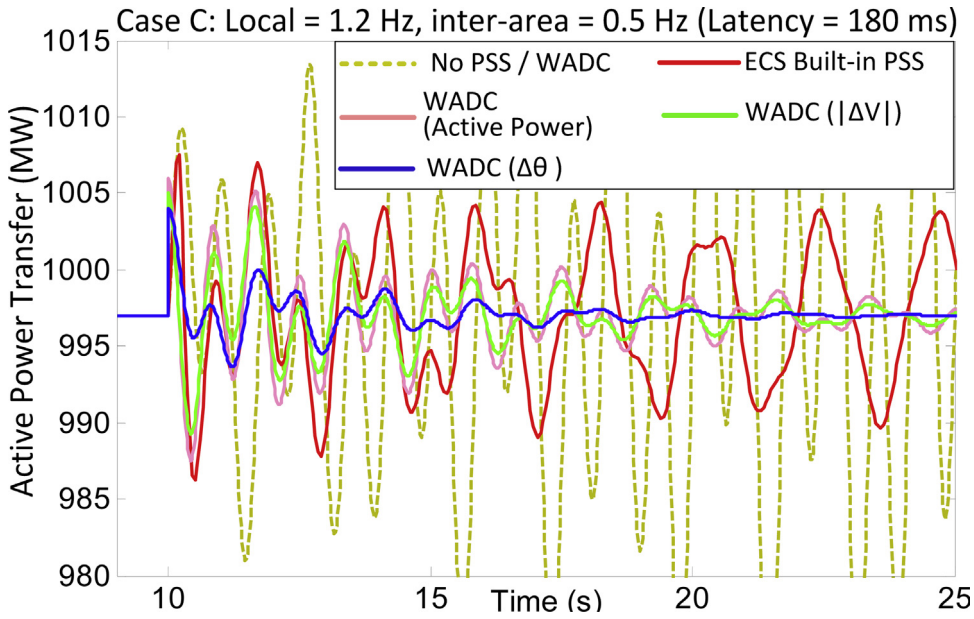

Fig. 14. Experimental results: 1.2 Hz local mode and 0.5 Hz inter-area mode damping using the internal-PSS and external damping signals from WADC.

Table 3
Case C: parameter configuration of POD algorithm (multiple modes).

Parameter		WADC active [ower	WADC $\|\Delta V\|$	WADC $\|\Delta\theta\|$
Phase shift	β_1	90^0	180^0	90^0
	β_2	90^0	180^0	90^0
Gain	K_{POD1}	0.001	1.1	0.02
	K_{POD2}	0.002	2.3	0.05

Table 4
Case C: time domain performance metrics (multiple modes).

Damping signal	Decay ratio	Overshoot (%)	Rise time (s)	Setting time (s)
Built-in PSS	1.015	Unstable	Infinity	Infinity
WADC active power	0.997	1.17	0.42	1.76
WADC $\|\Delta V\|$	0.992	0.71	0.24	0.58
WADC $\Delta\theta$	0.983	0.70	0.20	0.26

is only one oscillatory mode (Fig. 11, red trace), and its performance degrades when multiple oscillatory modes are present (Fig. 14, red trace). This is because for Case-C (multiple oscillatory modes), the parameters of the internal PSS of ECS were tuned for local mode of 1.2 Hz. As a result, the 0.5 Hz inter-area oscillatory mode does not damp and remains visible in the active power transfer through the transmission line (Fig. 14, red trace).

All the synchrophasors-based external damping signals from the WADC, when supplied to the ECS, provide adequate damping for both single and multiple oscillatory modes. As shown in Table 2 for Case-A (single mode), the damping capability of ECS when supplied with external signals from the WADC is comparable with its internal PSS. However, the damping capability of ECS for multiple oscillatory modes (Case-C) improves significantly when supplied with external damping signals from the WADC as shown in Fig. 14 and Table 4. This is because the WADC generates damping signals

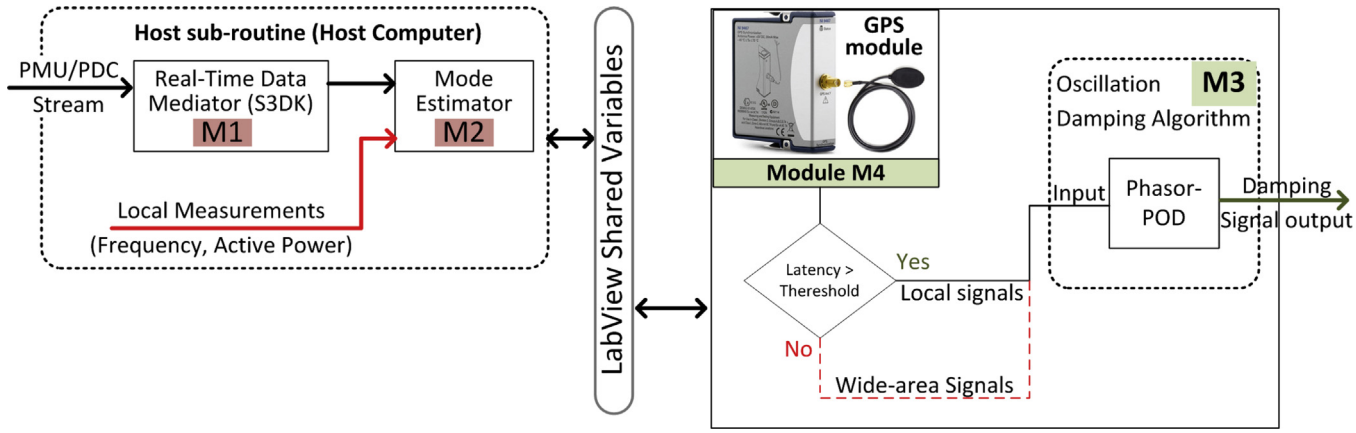

Fig. 15. WADC architecture exploitation to incorporate resiliency to communication loss.

based on oscillatory contents extracted from both inter-area and local modes.

Figs. 11 and 14 reveal that using voltage phase angle difference measurement as feedback input signal to the WADC is an effective means for damping both single (inter-area) and multiple (inter-area and local) oscillatory modes. This is because the observability of the modes of interest is the maximum in the voltage phase angle difference measurement [34], which increases the performance of the WADC controller that feeds damping signals to the ECS. This shows, experimentally, that utilizing synchrophasor measurements from remote locations provide new options for selection of the best feedback signal for oscillation damping.

7. Discussion

In actual hardware deployment, a number of factors need to be considered. Some of these are:

1. Operational limits of the equipment: As the hardware WADC is interfaced with both real-time simulator and ECS, which have different limits for the input/output signal, therefore appropriate signal scaling needs to be performed to make sure that the signal remains within the limits (I/Os, operational limits of interfacing amplifiers etc.) during operation. For example the range of the analog output of the simulator is ±10 V and ±20 mA, which should not be exceeded in any conditions (e.g. in case of faults).
2. Signal noise: The frequent signal scaling coupled with the measurement noise integrated in the signal due to several hardware interfaces (between real-time simulator, amplifier, PMU, WADC and ECS) deteriorates the overall signal and effects the performance of the WADC.
3. Computation capability of WADC/hardware: Another constraint towards prototyping of real-time controllers is the computation capability (resourcefulness) of the hardware on which the control application is deployed. These resource-constrained embedded controllers put a limit on the complexity of the algorithm/code that can be executed in them.

These constraints/complexities are apparent during hardware prototyping of the controller and can result in disparate performance of the deployed hardware as compared to its simulation-alone results. This study aims to bridge the gap between damping controller designs (where plethora of research is carried out), and their real-field deployment by making the implementation part more transparent. The simulation-only exercises in power system CAD software provide no realistic insight into actual design and implementation challenges.

With the currently available commercial ECS, power system operators cannot select any wide-area measurements as an input damping signal to AVRs. The limitation is due to the fact that the built-in PSS implementation in the ECS only allows using local input measurements which are not user selectable. In this study, the built-in PSS2B (of Unitrol 1020 ECS) is pre-configured to generate stabilizing signals using active power "P" and the frequency "f" at the terminals of the synchronous machine. The only liberty provided to the user is to tune the parameters of the lead-lag filters. The proposed approach enables bypassing the built-in PSS function in the ECS and gives more freedom to the end-user to utilize custom stabilizer models and/or wide-area signals (instead of local signals).

The proposed architecture enables the WADC to utilize any wide-area measurement to generate damping signal. In case of loss of communication, the WADC can utilize the local measurements (frequency, active power at the generators terminal) to generate damping signal. The local measurements can be sent to the WADC through communication network (using TCP/UDP) or by hardwired (using analog input module in the WADC). In these scenarios, the communication latency module (M4) can be configured with a threshold value (for the signal latency T_d) to switch from wide-area signal to the local signal-based damping. The user/operator can then remotely tune the parameters of the WADC to provide adequate damping using local measurements. Graphical representation of such a scheme is shown in Fig. 15.

8. Conclusion

The study shows that synchrophasor-based damping signals can be fed to the commercial ECS to provide adequate damping to power system oscillations. This is demonstrated through RT-HIL simulation experiments using commercial PMUs, a hardware prototype of wide-area damping controller (WADC) and a commercially available Excitation Control System (ECS). Case studies confirm the effectiveness of the proposed technique, both in terms of identifying critical oscillatory modes, and compensation for communication latency associated with synchrophasors. This method provides an opportunity to exploit existing ECS together with synchrophasor technology, without substantially modifying the associated electrical installation. Furthermore, the method allows real-time monitoring and remote tuning of WADC parameters before supplying them to the ECS, which enables (TSOs) to generate damping signals adaptive to the changes in operating conditions or network topology. The modular architecture and the deployment method can be utilized to prototype any synchrophasor-based wide-area control application.

Acknowledgements

The support of the following funding bodies is gratefully acknowledged: Nordic Energy Research through the STRONg^{2}rid project; Statnett SF, the Norwegian Transmission System Operator, through projects Symptom and RT-VS; The STandUP for Energy collaboration initiative, through the SRA grant. KTH SmarTS-Lab would like to thank ABB Switzerland AG for their donation of Unitrol 1020 Excitation Control System.

References

[1] F.P. deMello, C. Concordia, Concepts of synchronous machine stability as affected by excitation control, IEEE Trans. Power Appar. Syst 88 (4) (1969) 316–329.
[2] E.V. Larsen, D.A. Swann, Applying power system stabilizers, IEEE Trans. Power Appar. Syst. PAS-100 (June) (1981) 3017–3041.
[3] F.P. deMello, T.F. Laskowski, Concepts of power system dynamic stability, IEEE Trans. Power Appar. Syst. 94 (1979) 827–833.
[4] M. Klein, G. Rogers, P. Kundur, A fundamental study of inter-area oscillations in power systems, IEEE Trans. Power Syst. 6 (3) (1991) 914–921.
[5] A. Bose, Smart transmission grid application and their supporting infrastructure, IEEE Trans. Smart Grid 1 (2010) 11–19.
[6] Y. Chompoobutrgool, L. Vanfretti, Using PMU signals from dominant paths in power system wide-area damping control, Sustain. Energy Grids Netw. 4 (October) (2015) 16–28.
[7] J. Chow, J. Sanchez-Gasca, H. Ren, S. Wang, Power system damping controller design-using multiple input signals, IEEE Control Syst. Mag. 20 (August (4)) (2000) 82–90.
[8] I. Kamwa, et al., Wide-area measurement based stabilizing control of large power systems—a decentralized/hierarchical approach, IEEE Trans. Power Syst. 16 (February (1)) (2001) 136–153.
[9] Y. Zhang, A. Bose, Design of wide-area damping controllers for interarea oscillations, IEEE Trans. Power Syst. 23 (August (3)) (2008) 1136–1143.
[10] I. Kamwa, et al., Optimal integration of disparate C37.118 PMUs in wide-area PSS with electromagnetic transients, IEEE Trans. Power Syst. 28 (November (4)) (2013) 4760–4770.
[11] X. Xie, J. Xiao, C. Lu, Y. Han, Wide-area stability control for damping interarea oscillations of interconnected power systems, IEE Proc.: Gener. Transm. Distrib. 153 (5) (2006) 507–514.
[12] R. Preece, J.V. Milanović, A.M. Almutairi, O. Marjanovic, Damping of inter-area oscillations in mixed AC/DC networks using WAMS based supplementary controller, IEEE Trans. Power Syst. 28 (May (2)) (2013) 1160–1169.
[13] B. Chaudhuri, B.C. Pal, Robust damping of multiple swing modes employing global stabilizing signals with a TCSC, IEEE Trans. Power Syst. 19 (February (1)) (2004) 499–506.
[14] N.R. Chaudhuri, B. Chaudhuri, S. Ray, R. Majumder, Wide-area phasor power oscillation damping controller: a new approach to handling time-varying signal latency, IET Gener. Transm. Distrib. 4 (May (5)) (2010) 620–630.
[15] K. Uhlen, et al., Wide-area power oscillation damper implementation and testing in the Norwegian transmission network, IEEE Power and Energy Society General Meeting (2012).
[16] C. Lu, et al., Implementations and experiences of wide-area HVDC damping control in China southern power grid, in: IEEE Power and Energy Society General Meeting, San Diego, CA, 2012.
[17] B. Pierre, et al., Supervisory system for a wide area damping controller using PDCI modulation and real-time PMU feedback, in: IEEE Power and Energy Society General Meeting, Boston, MA, 2016.
[18] R. Preece, Improving the Stability of Meshed Power Networks, Springer Inc., New York, 2013, ch. 1, sec. 1.3.1.2, pp. 12.
[19] CIGRE Task Force 38.02.16, Impact of Interactions among Power System Controllers, CIGRE, Nov. 1999.
[20] M.J. Gibbard, D.J. Vowles, P. Pourbeik, Interactions between, and effectiveness of, power system stabilizers and FACTS device stabilizers in multi-machine systems, IEEE Trans. Power Syst. 15 (May (2)) (2000) 748–755.
[21] ABB-Unitrol 1020 Automatic Voltage Regulator. Available online: http://tinyurl.com/Unitrol.
[22] IEEE Standard 421.5-2005, IEEE Recommended Practice for Excitation System Models for Power System Stability Studies, 2006.
[23] WECC, Power System Stabilizer (PSS) Design and Performance, WECC Regional Reliability Standard, VAR-501-WECC-3—Power System Stabilizers, January, 2016. Available online: https://www.wecc.biz.
[24] L. Angquist, C. Gama, Damping algorithm based on phasor estimation, IEEE PES Winter Meeting vol. 3 (2001) 1160–1165.
[25] L. Vanfretti, et al., A Software Development Toolkit for Real-Time Synchrophasor Applications, IEEE Powertech, France, 2013, June.
[26] IEEE Standard for Synchrophasor Data Transfer for Power Systems, IEEE C37.118.2-2011, IEEE Power and Energy Society, December, 2011.
[27] P. Anderson, R. Brinker, The stochastic subspace identification techniques, in: Proc. 24th Int. Modal Anal. Conf., Missouri, 2006.
[28] J.-N. Juang, R.S. Pappa, An eigensystem realization algorithm for modal parameter identification and model reduction, J. Guid. Control Dyn. 8 (September (5)) (1985) 620–627.
[29] M. Baudette, et al., 'In silico' testing of a real-time PMU-based tool for power system mode estimation, in: IEEE PES GM, Boston, 2016.
[30] National Instruments, Operating Instructions and Specifications Compact RIO NI-cRIO 9081/9082.
[31] E. Rebello, L. Vanfretti, M.S. Almas, PMU-based real-time damping control system software and hardware architecture synthesis and evaluation, in: IEEE PES GM, Denver, CO, July, 2015.
[32] National Instrument, Labview-System Design Software. Available online: http://www.ni.com/labview/.
[33] Opal-RT, eMEGAsim PowerGrid Real-Time Digital Hardware in the Loop Simulator, Available online: http://www.opal-rt.com/.
[34] L. Vanfretti, Y. Chompoobutrgool, J.H. Chow, Chapter 10: inter-area mode analysis for large power systems using synchrophasor data, book chapter, in: Joe H. Chow (Ed.), Coherency and Model Reduction of Large Power Systems, Springer, 2013.